Semi-Annual Status Report

IMPROVEMENTS IN THE GLOBAL REFERENCE ATMOSPHERIC MODEL AND COMPARISONS WITH A GLOBAL 3-D NUMERICAL MODEL

C. G. Justus, Principal Investigator
F. N. Alyea, D. M. Cunnold and George Chimonas, Co-Investigators
School of Geophysical Sciences
Atlanta, Georgia 30332-0340

April, 1989

Report Period: September 23, 1988 - March 22, 1989

Prepared for the

NATIONAL AERONAUTICS AND SPACE ADMINISTRATION
MARSHALL SPACE FLIGHT CENTER

Under Grant No. NAG8-078

Georgia Tech Project G-35-685

STATUS OF THE GLOBAL REFERENCE ATMOSPHERIC MODEL (GRAM)

All of the data from a variety of sources has been analyzed and new "SCIDAT" data file listings for the revised zonal mean values, stationary perturbation values, and random perturbation values have been sent to Marshall Space Flight Center for review and comment. Barring any recommended changes, these data will become the new "SCIDAT" data (along with previous, unchanged values for the NMC grid point locations, the annual fractional variances in the large scale perturbations, the velocity-density correlation values, and the quasi-biennial parameter values).

During the coming period the programming modifications to GRAM will be implemented and tested. These changes, along with the revised "SCIDAT" data will become the new, revised GRAM-90 model. The programming changes required are mostly to accommodate the new, higher resolution, stationary perturbation values, and the new zonal mean and stationary perturbations for mean wind components (to replace the spherical harmonic wind model in the middle atmosphere altitude range).

Following the program modifications, height-latitude cross-sectional contour plots will be generated, to compare with comparable cross-sections evaluated from the stratospheric global circulation model of Drs. Alyea and Cunnold. The equivalent contours from the current GRAM (GRAM-88), have previously been evaluated and will be compared to demonstrate changes and improvements between the GRAM-88 and GRAM-90 model versions.

STATUS OF THE MARS GLOBAL REFERENCE ATMOSPHERIC MODEL (MARS-GRAM)

Following a long history of development and improvement of the Global Reference Atmospheric Model (GRAM) for the atmosphere of Earth (Justus, et al., 1975, 1976; Justus and Roper 1987; Justus, 1988), NASA, under grant monitorship by Marshall Spaceflight Center, has commissioned Georgia Tech to develop a similar model, the Mars Global Reference Atmosphere Model (MARS-GRAM) for the atmosphere of that planet. MARS-GRAM, is based on parameterizations to approximate, as realistically as possible, the temperature, pressure, density and winds of the Martian atmosphere, and their latitudinal, longitudinal, diurnal, seasonal and altitude variation, from the surface through thermospheric altitudes. Parameterizations are also included for the effects of global-scale dust storms on the variations of the thermodynamic and wind properties of the Martian atmosphere. Recently, David Kaplan, compiler of the definitive report "Environment of Mars, 1988" (Kaplan, 1988), has decided to propose MARS-GRAM as the reference model atmosphere for use by engineers on upcoming equipment design contracts for NASA's Mars Rover and Sample Return Mission (Kaplan, private communication).

The near-surface air temperature on Mars is parameterized in the MARS-GRAM program by computing an approximate value for the geographically and seasonally-dependent daily total absorbed radiation flux. The daily average, maximum and minimum near-surface air temperatures are then calculated from a simple regression relationship assumed between the daily absorbed flux and the temperature parameters. The absorbed flux estimates include the variations in insolation due to the orbital position of Mars, the latitudinal variation of surface albedo (Pollack, et al. 1981), and seasonally-dependent parameterizations for the polar caps (Martin and James, 1986a, 1986b; Iwasaki, 1986; Paige and Ingersoll, 1985; Philip, 1986) and polar hood clouds (James et al., 1987). The resultant seasonally and latitudinally dependent daily

average, maximum and minimum temperatures from the MARS-GRAM model are shown in Figures 1-3. These agree well with the surface temperature maps of Kieffer et al. (1977), with more realistic variations in the polar regions, as suggested by the observations of Kieffer (1979). Seasonal variations of the daily maximum, minimum and average temperature at the latitudes of the Viking 1 and Viking 2 landers, as evaluated by MARS-GRAM, are shown in Figures 4a and 5a. These plots agree nicely with the Viking 1 and Viking 2 observational data reported by Ryan and Henry (1979), shown for comparison in Figures 4b and 5b.

MARS-GRAM parameterizations for the geographical, seasonal and altitude dependence of non-dust storm, daily average temperatures above the surface come from a combination of observational and model values. The observational data include: Mariner 9 IRIS data from Conrath (1981), and Conrath data as reported by Leovy (1982) and Magalhaes (1987), Viking IRTM data (Martin et al., 1982), Mariner 9 radio occultation data from Kliore (1973), and Viking 1 radio occultation data (Fjeldbo et al., 1977), Lindal et al. (1979), and Davis et al. (1979). Model output used include results from Pollack et al. (1981), Haberle et al. (1982), and Pitts et al. (1988). An example of the altitude dependence of the non-dust storm daily average temperatures from MARS-GRAM is shown in Figure 6, for Northern Hemisphere winter solstice (areocentric longitude of sun, $L_s = 270°$).

The parameterizations in MARS-GRAM for temperature variations during dust storm conditions were taken from observational data of Kliore et al. (1972), Jakosky and Martin (1987), Martin et al. (1982), Hanel et al. (1972), and Cornrath (1975). Model values for dust storm effects were taken from Haberle et al. (1982) and Pitts et al. (1988). An example of a MARS-GRAM dust-storm temperature cross section (at $L_s = 270°$) is shown in Figure 7.

Data for the MARS-GRAM parameterizations of the height variation of the diurnal (longitudinal) variations of temperature about the daily mean value were taken from Viking IRTM observations of Martin et al. (1982), Mariner 9 IR spectroscopy data of Hanel et al. (1972), and model results from Zurek, as reported in Pitts et al. (1988). Diurnal temperature variations (not shown here) are significantly larger during dust storm periods than during non-dust storm conditions.

The new parameterizations for MARS-GRAM provide a simulation capability to altitudes reaching the base of the thermosphere. For simulations of the seasonal, geographical and solar-activity dependence of thermospheric conditions, the MARS-GRAM uses an adaption of the thermospheric model of Stewart (Culp and Stewart, 1983, 1984; Stewart and Hanson, 1982; Stewart, 1987; see also the revised Stewart program code given in Pitts et al., 1988).

The MARS-GRAM has numerous applications as a "poor man's global circulation model". For example, the computation of all of the data necessary to describe the complete seasonal variations at the surface (Figures 1-3) and all altitudes (e.g. Figure 8), takes at most a few minutes on an IBM-PC (with 8087 co-processor; even faster on an IBM-AT or a 80386-based PC). Comparable data would take many hours of computation on a mainframe using a 3-D global circulation model for Mars. The diurnal (longitudinal) variability incorporated into the MARS-GRAM program is not even available in a 2-D version of a Mars global circulation model.

In addition to the engineering applications envisioned for MARS-GRAM (e.g. aerocapture mission profile studies, Mars Rover Sample return mission planning and design), the MARS-GRAM has a number of potential scientific applications. One of these is its ability to provide a realistic,

geographically and seasonally-dependent background of temperatures and winds for studies of tides and the atmospheric propagation of other wave disturbances (e.g. gravity waves, mountain lee waves, etc.). Another application would be in providing realistic "first guess" profiles for the inversion processing for temperature retrievals from temperature sounders on upcoming Mars missions.

Of course, being a parameterization model, rather than a first principles one such a global circulation model, MARS-GRAM is only as good as the parameterizations built into it. Also it cannot test the sensitivity to variation of parameters beyond those on which the parameterizations are based (e.g. it cannot estimate the effects of a dust storm of twice the optical depth previously observed). With continued analysis of additional observational data from the Viking and Mariner programs, analysis of new results from global circulation models, and with new data expected to be coming in from the Mars Observer program, MARS-GRAM should steadily improve in its realism and reliability in the future.

WAVES IN THE MARTIAN ATMOSPHERE

Wave-like perturbations have been observed in the Viking 1 and Viking 2 surface pressure data (Leovy, 1981), in the Mariner 9 IR spectroscopy data (Pirraglia and Cornrath, 1974; Cornrath, 1976, 1981), and in the Viking 1 and Viking 2 lander entry profiles (Seiff and Kirk, 1976, 1977). Most of the wave-like perturbations have been interpreted as atmospheric tides (Pirraglia and Cornrath, 1974; Cornrath, 1976; Seiff, 1982), or as planetary waves (Cornrath, 1981; Barnes and Hollingsworth, 1988). The theory of thermal tides in the Martian atmosphere has been well explored (Zurek, 1976, 1986; Zurek and Haberle, 1988). Compared to the detailed tidal analyses, relatively little attention has been paid to other forms of wave perturbations, such as gravity waves (Gadian and Green, 1983), Kelvin waves and normal modes (Zurek, 1988; Hamilton et al., 1986; Tilman, 1988), and lee waves (Pickersgill and Hunt, 1979). The very strong influence of topography on the wave structure in the Martian atmosphere has been documented both by observational data (Cornrath, 1976) and by theoretical analysis (Zurek, 1976).

One of the best-known properties of gravity waves is that their amplitudes increase with height as the inverse square root of the mean atmospheric density. In this way, the kinetic energy of the wave is maintained even as the packet propagates upward into the rarer regions. The effect has been likened to the wave-kink that grows as it travels along a whip from the thick end near the handle to the thin region near the tip. The comparison is even more apt than first appears, for just as the wave traveling up the whip reaches an unsustainable amplitude and "cracks", the gravity wave may reach heights at which it becomes too large for smooth fluid behavior and it turns over into shocks and/or turbulence.

One of the common sources of gravity waves is wind flow over mountains. As the atmospheric flow reaches the mountain, surface pressures deflect it up and over the mountain rise, and then restore it to level on the other side. However, the disturbance transmitted to the air flow is not confined to some surface region, as the pressure fields associated with the deflection have space and time scales that match the characteristics of gravity waves in the free atmosphere. Distorting any elastic medium in a way that matches its natural modes causes the excitation of waves that broadcast energy from the disturbance to the far reaches of the medium. So, around mountainous regions

the atmosphere normally contains a wealth of wave activity. Mountain waves, especially the resonant forms known as lee waves, are a familiar phenomenon of the Earth's atmosphere, and are expected to be of even more importance in the Martian atmosphere.

Because erosion is much weaker in the rainless Martian environment, and because surface gravity is lower, surface features on Mars tend to be more severe than on Earth. Ridges and mountains are higher, while surface winds are comparable (and, at times, higher), so the Martian mountain waves provide stronger aerodynamic disturbances than are encountered on Earth.

The waves of most interest for aerobraking or lander vehicles are readily modeled by the long-wave approximation. This component of the disturbance maps up through the atmosphere as a replica of the underlying terrain, and, in common with all gravity waves, the associated fractional density disturbances grow ever greater with altitude. Effectively the probing spacecraft will be "flying into the mountains", even when it is several tens of kilometers above the peaks. Limits may be imposed by wave saturation, absorption by critical layers, or by dissipation of the waves by molecular viscosity, but over the larger terrain features the tops of these ghost mountains may occur as shocks or wedges of turbulence.

In the long-wave approximation, we assume that the wavenumber k satisfies the inequality

$$k^2 \ll N^2/U^2 \quad , \tag{1}$$

where N is the Brunt-Vaisala frequency, and U is the mean wind speed. Under this assumption the governing differential equation for wave perturbations is

$$d^2y/dz^2 + [N^2/U^2 - (d^2U/dz^2)/U - 1/4H^2]y(z) = 0 \quad , \tag{2}$$

where H is the atmospheric scale height. The Fourier transform, $\hat{w}(z)$, for the vertical velocity perturbations is, for example, given by

$$\hat{w}(z) = \rho_o(z)^{-1/2} A(k)\, y(z) \quad , \tag{3}$$

where ρ_o is the mean density, A(k) is presently an unknown Fourier amplitude, and y(z) is the solution obtained from equation (2).

The assumption of purely tangential flow for the surface boundary condition determines the wave amplitude in terms of the slope dh/dx of the surface terrain and the mean wind speed U(0) that must be deflected over the terrain undulation. The Fourier transform of this surface condition defines the component amplitudes A(k) of equation (3) through the Fourier components of the surface terrain shape, h(x).

From this approach, the Fourier transform of the density variations can be obtained. Since there is no k dependence for the coefficients relating the Fourier transform of the density to the Fourier transform of the terrain surface, the Fourier inversion to obtain the vertical profile of density perturbations is straightforward, and yields

$$\rho_w(x,z)/\rho_o = \left[\frac{y(z)U(0)N^2}{y(0)U(z)g}\left[\frac{\rho_o(0)}{\rho_o(z)}\right]^{1/2}\right]h(x) \quad . \tag{4}$$

The implications of equation (4) are clear:

(a) The horizontal structure of the density disturbance ρ_w is an image of the terrain shape h(x).

(b) There is the standard vertical growth factor associated with gravity waves, proportional to the inverse square root of the mean density.

(c) There is a vertical wave structure y(z)/y(0), which will usually be closely sinusoidal.

(d) There is an excitation factor $[U(0)N^2/U(z)g]$ relating surface conditions to the generated wave density field.

These results apply equally to an isolated surface feature, such as a mountain sitting alone in the plains region, or an extended complex area of severe terrain. If the surface shape is known, and one differential equation involving the meteorological functions U(z) and N(z) is solved, the density perturbation, $\rho_w(x,z)$, at any location above the surface is obtained. Although derived here for the two-dimensional case, the results of equation (4) can easily be generalized to a fully three-dimensional terrain description.

It is proposed that a study of mountain waves in the Martian atmosphere be carried out, with the MARS-GRAM model providing the information on background profiles of U(z) and N(z). For these studies, terrain elevations relative to the reference ellipsoid of Cain et al. (1973), will be used (as revised from Viking measurements). As the wave amplitudes grow sufficiently large, wave "saturation" effects or wave breaking can occur. Although the linear theory considered here does not allow exact solutions under such circumstances, the theory, in conjunction with the MARS-GRAM profiles of U(z) and N(z), will allow the determination of the altitudes at which such saturation and breaking processes are likely to occur, and what magnitude of energy deposition is likely to be associated with these phenomena.

If non-linear processes do not limit the growth of the wave, the high kinematic molecular viscosity of the upper atmosphere will. Because of lower density, the molecular viscosity effect will be felt at lower altitudes on Mars than on Earth. The treatment of Pitteway and Hines (1963), can be used to model this effect.

MARS-GRAM PLANS FOR THE COMING PERIOD

During the coming period, a version of the MARS-GRAM program, suitable for engineering use will be completed. It will include the temperature variations discussed here. Latitudinal and seasonal variations in surface pressure (including parameterized dust-storm perturbations, when desired) will be included. Surface pressure and temperature profile information will be

used in hydrostatic and perfect gas law relationships to construct profiles of pressure and density up to thermospheric altitudes, where the profiles will be smoothly merged into the latest version of the Stewart thermospheric model. Winds in the MARS-GRAM model will be evaluated with a thermal wind (areostrophic wind) approximation, with a modification to account for large values of kinematic molecular viscosity (as in the current MARS-GRAM). A simple version of the wave perturbation model of Dr. Chimonas, discussed above, will be implemented as a replacement model for the density perturbation magnitudes in the MARS-GRAM, at least up to thermospheric altitudes.

REFERENCES

Barnes, Jeffrey R. Jeffery L. Hollingsworth (1988). Dynamical Modeling of a Planetary Wave Mechanism for a Martian Polar Warming. Icarus, 71(2): 313-334

Cain, D.L., A.J. Kliore, B.L. Seidel, M.J. Sykes, and P. Woiceshyn (1973). Approximations to the Mean Surface of Mars and Mars Atmosphere Using Mariner 9 Occultations. J. Geophys. Res., 78(20): 4352-4354

Conrath, Barney J. (1975). Thermal Structure of the Martian Atmosphere during the Dissipation of the Dust Storm of 1971. Icarus, 24: 36-46

Conrath, Barney J. (1976). Influence of Planetary-Scale Topography on the Diurnal Thermal Tide During the 1971 Martian Dust Storm. J. Atmos. Sci., 33: 2430-2439

Conrath, Barney J. (1981). Planetary-Scale Wave Structure in the Martian Atmosphere. Icarus, 48: 246-255

Culp, Robert D., A.I. Stewart, Chia-chuan Chow (1983). Time Dependent Model of the Martian Atmosphere for use in Orbit Lifetime and Sustenance Studies. JPL Contract #956446: Univ. of Colorado, 31 pp.

Culp, Robert D., and A. Ian Stewart (1984). Time-Dependent Model of the Martian Atmosphere for Use in Orbit Lifetime and Sustenance Studies. J. Astron. Sci., 32(3): 329-341

Davies, D. W. (1979). The Relative Humidity of Mars' Atmosphere. J. Geophys. Res., 84: 8335

Fjeldbo, Gunnar, Donald Sweetnam, Joseph Brenkle, Edward Christensen, David Farless, et al (1977). Viking Radio Occultation Measurements of the Martian Atmosphere and Topography: Primary Mission Coverage. J. Geophys. Res., 82(28): 4317-4324

Gadian, A.M., and J.S.A. Green (1983). A Theoretical Study of Small Amplitude Waves in the Martian Lower Atmosphere and a Comparison Made with Those on Earth. Annales Geophysicae, 1(3): 239-244

Haberle, Robert M., Conway B. Leovy, and James B. Pollack (1982). Some Effects of Global Dust Storms on the Atmospheric Circulation of Mars. Icarus, 50: 322-367

Hamilton, Kevin, and Rolando R. Garcia (1986). Theory and Observations of the Short-Period Normal Mode Oscillations of the Atmosphere. J. Geophys. Res., 91(D11): 11867-875

Hanel, R., B. Conrath, W. Hovis, V. Kunde, P. Lowman, W. Maguire, J. Pearl, et al. (1972). Investigation of the Martian Environment by Infrared Spectroscopy on Mariner 9. Icarus, 17: 423-442

Iwasaki, K, et al. (1986). Interannual Differences of Mars Polar Caps. MECA Symposium on Mars: Evolution of Its Climate and Atmosphere, LPI Tech. Rept. 87-01: 58-59

Jakosky, Bruce M., Terry Z. Martin (1987). Mars: North-Polar Atmospheric Warming During Dust Storms. Icarus, 72: 528-534

James, Philip B., Maurice Pierce, Leonard J. Martin (1987). Martian North Polar Cap and Circumpolar Clouds: 1975-1980 Telescopic Observations. Icarus, 71: 306-312

Justus, C. G., R. G. Roper, Arthur Woodrum, and O. E. Smith (1975). Global Reference Atmospheric Model for Aerospace Applications. J. Spacecraft and Rockets, 12: 449-450

Justus, C. G., R. G. Roper, Arthur Woodrum, and O. E. Smith (1976). A Global Reference Atmospheric Model for Surface to Orbital Altitudes. J. Appl. Meteorol., 15: 3-9

Justus, C. G. and R. G. Roper (1987). Application of the Global Reference Atmospheric Model to Polar Orbit Missions. AIAA 25th Aerospace Sciences Meeting, January, Reno, NV, paper AIAA-87-0264

Justus, C. G. (1988). Density Perturbation Simulation with the Global Reference Atmospheric Model. AIAA 26th Aerospace Science Meeting, January, Reno, NV, paper AIAA-88-0494

Kaplan, David (1988). Environment of Mars, 1988. NASA Tech. Memo 100470: October: 62 pp.

Kieffer, H. H. (1979). Mars South Polar Spring and Summer Temperatures: A Residual CO_2 Frost. J. Geophys. Res., 84(B14): 8263-8288

Kieffer, H. H., T. Z. Martin, A. R. Peterfreund, B. M. Jakosky, E. D. Miner, and F. D. Palluconi (1977). Thermal and Albedo Mapping of Mars During the Viking Primary Mission, J. Geophys. Res., 82: 4249-4291

Kliore, A.J., G. Fjeldbo, B.L. Seidel, M.J. Sykes, and P.M. Woiceshyn (1973). S Band Radio Occultation Measurements of the Atmosphere and Topography of Mars with Mariner 9: Extended Mission Coverage of Polar ... J. Geophys. Res., 73(20): 4331-4351

Kliore, Arvydas J., Dan L. Cain, Gunnar Fjeldbo, Boris L. Seidel, Michael J. Sykes, S.I. Rasool (1972). The Atmosphere of Mars from Mariner 9 Radio Occultation Measurements. Icarus, 17: 484-516

Leovy, C. (1982). Martian Meteorological Variability. Adv. Space. Res., 2: 19-44

Leovy, Conway B. (1981). Observations of Martian Tides Over Two Annual Cycles. J. Atmos. Sci., 38: 30-39

Lindal, G. F., et al. (1979). Viking Radio Occultation Measurements of the Atmosphere and Topography of Mars: Data Acquired During 1 Martian Year of Tracking. J. Geophys. Res., 84: 8443

Magalhaes, J. A. (1987). The Martian Hadley Circulation: Comparison of "Viscous" Model Predictions to Observations. Icarus, 70: 442-468

Martin, L. J. and P. B. James (1986a). Major Dust Storm Activity and Variations in the Recession of Mars' South Polar Cap. MECA Workshop on the Evolution of the Martian Atmosphere, LPI Tech. Rept. 86-07: 29-30

Martin, L. J. and P. B. James (1986b). The Great Dust Storm of 1986(?). MECA Workshop on Mars: Evolution of its Climate and Atmosphere. LPI Tech Rept. 87-01: 76-77

Martin, T.Z., M.M. Kieffer, and E.D. Miner (1982). Mars' Atmospheric Behavior from Viking Infra-red Thermal Mapper Measurements. Adv. Space Res., 2: 57-65

Paige, David A., Andrew P. Ingersoll (1985). Annual Heat Balance of Martian Polar Caps: Viking Observations. Science, 228: 1160-1168

Philip, J.R. (1986). Similarity Analysis of the Martian Polar Caps. Geophys. Res. Lett., 13(11): 1137-1140

Pickersgill, A. O. and G. E. Hunt (1979). The Formation of Martian Lee Waves Generated by a Crater. J. Geophys. Res., 84: 8317

Pirraglia, Joseph A., and Barney J. Conrath (1974). Martian Tidal Pressure and Wind Fields Obtained from the Mariner 9 Infrared Spectroscopy Experiment. J. Atmos. Sci., 31: 318-329

Pitteway, M.L.V. and C.O. Hines (1963). The Viscous Damping of Atmospheric Gravity Waves. Can. J. Phys., 41: 1935

Pitts, David E., James E. Tillman, James Pollack, Richard Zurek (1988). Model Profiles of the Mars Atmosphere for the Mars Rover and Sample Return Mission. Preprint.

Pollack, James B., Conway B. Leovy, Paul W. Greiman, and Yale Mintz (1981). A Martian General Circulation Experiment with Large Topography. J. Atmos. Sci., 38(1): 3-29

Ryan, J. A. and R. M. Henry (1979). J. Geophys. Res., 84: 2821-2829

Seiff, A. (1982). Post-Viking Models for the Structure of the Summer Atmosphere of Mars. Adv. Space. Res., 2: 3-17

Seiff, Alvin, and Donn B. Kirk (1976). Structure of Mars' Atmosphere up to 100 Kilometers from the Entry Measurements of Viking 2. Science, 194: 1300-1302

Seiff, Alvin, and Donn B. Kirk (1977). Structure of the Atmosphere of Mars in Summer at Mid-Latitudes. J. Geophys. Res., 82(28): 4364-4378

Stewart, A.I., and W.B. Hanson (1982). Mars' Upper Atmosphere: Mean and Variations. Adv. Space Res., 2: 87-101

Stewart, A.I.F. (1987). Revised Time Dependent Model of the Martian Atmosphere for use in Orbit Lifetime and Sustenance Studies. Final Report JPL PO# NQ-802429, March 26: 52 pp.

Tillman, James E. (1988). Mars Global Atmospheric Oscillations: Annually Synchronized, Transient Normal-Mode Oscillations and the Triggering of Global Dust Storms. J. Geophys. Res., 93(D8): 9433-9451

Zurek, Richard W. (1976). Diurnal Tide in the Martian Atmosphere. J. Atmos. Sci., 33: 321-337

Zurek, Richard W. (1986). Atmospheric Tidal Forcing of the Zonal-Mean Circulation: The Martian Dusty Atmosphere. J. Atmos. Sci., 43(7): 652-670

Zurek, Richard W. (1988). Free and Forced Modes in the Martian Atmosphere. J. Geophys. Res., 93(D8): 9452-9462

Zurek, Richard W., Robert M. Haberle (1988). Zonally Symmetric Response to Atmospheric Tidal Forcing in the Dusty Martian Atmosphere. J. Atmos. Sci., 45(18): 2469-2479

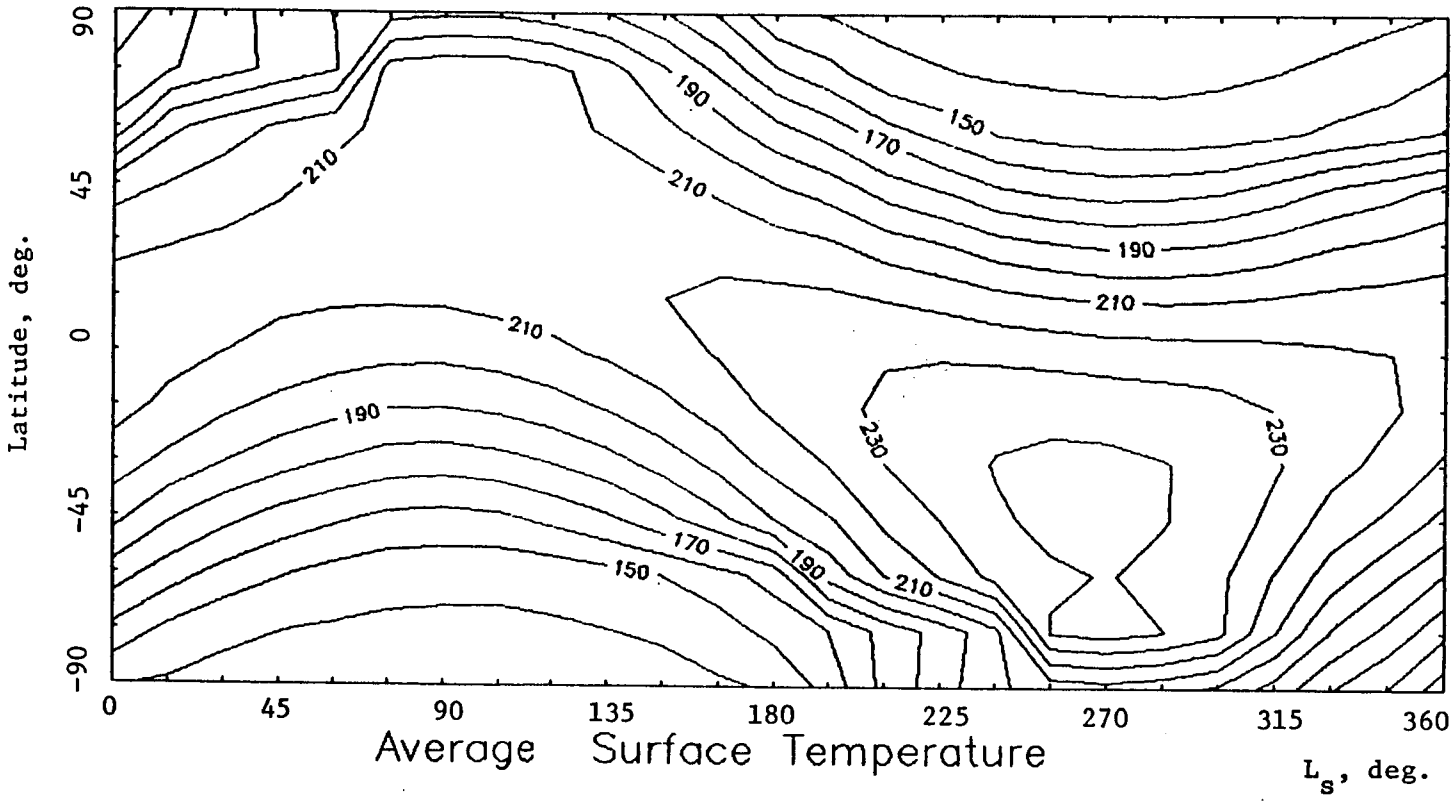

Figure 1 - Seasonal and latitudinal variation of daily average surface temperature, computed by the MARS-GRAM model. L_s is the areocentric longitude of the sun.

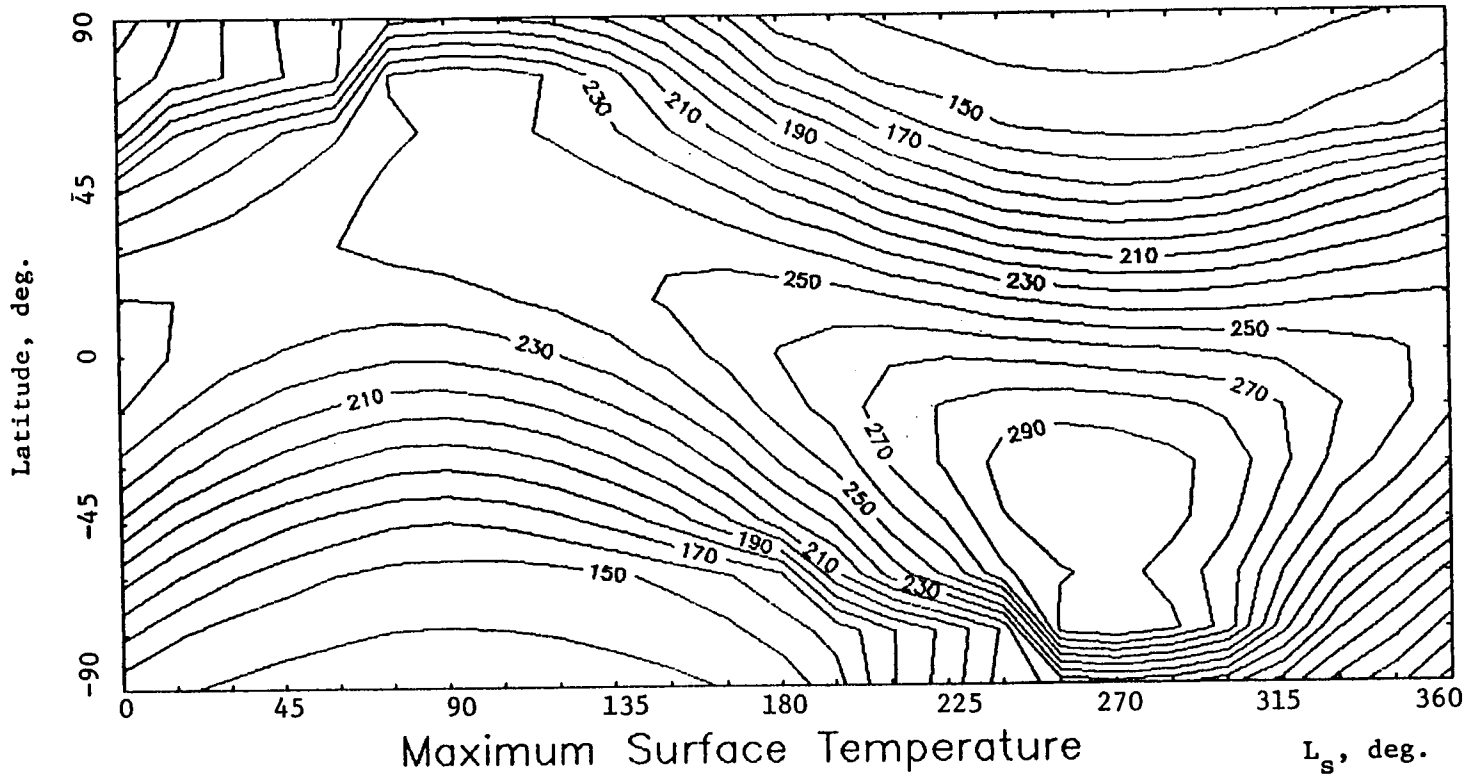

Figure 2 - Seasonal and latitudinal variation of daily maximum surface temperature, computed by the MARS-GRAM model.

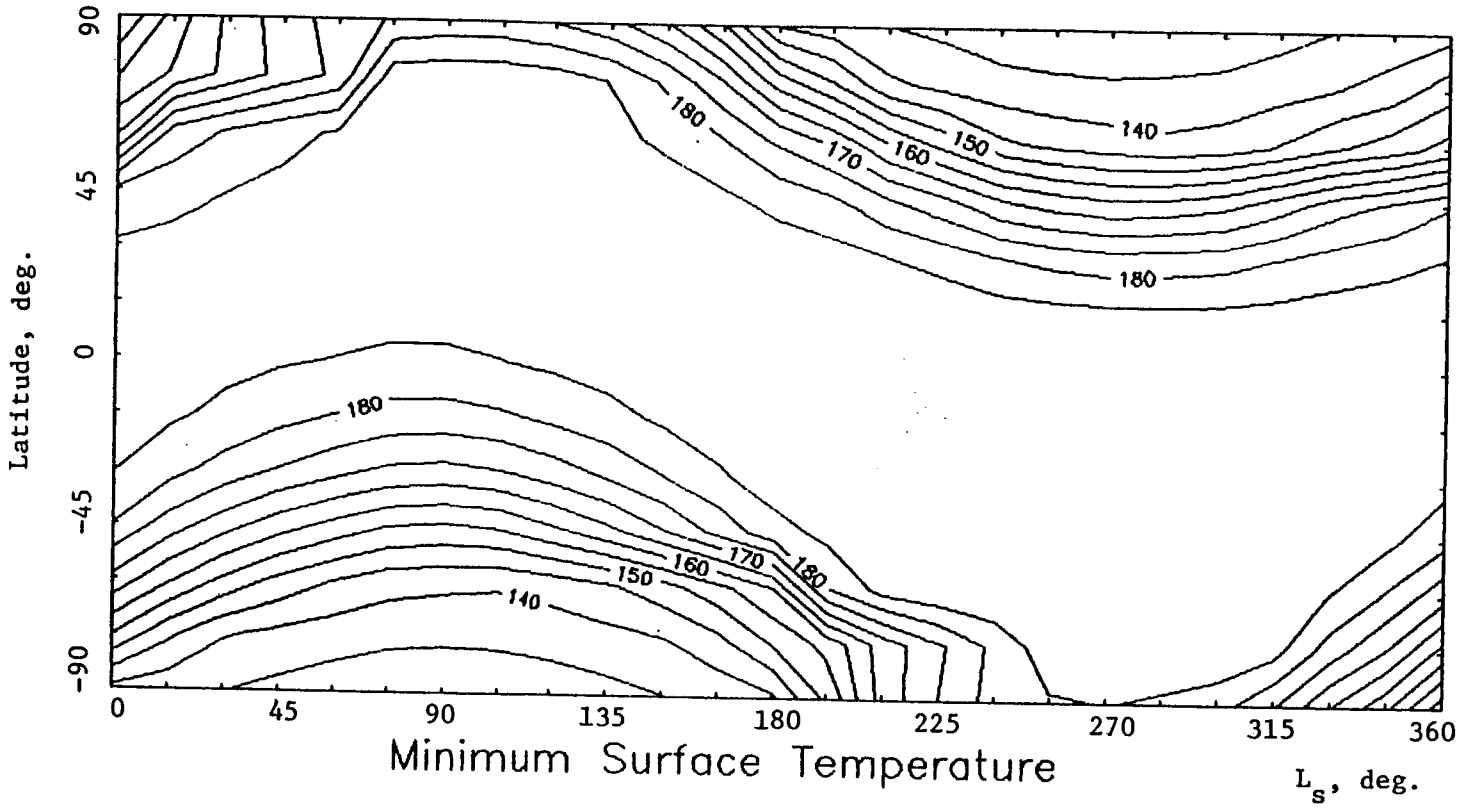

Figure 3 - Seasonal and latitudinal variation of daily minimum surface temperature, computed by the MARS-GRAM model.

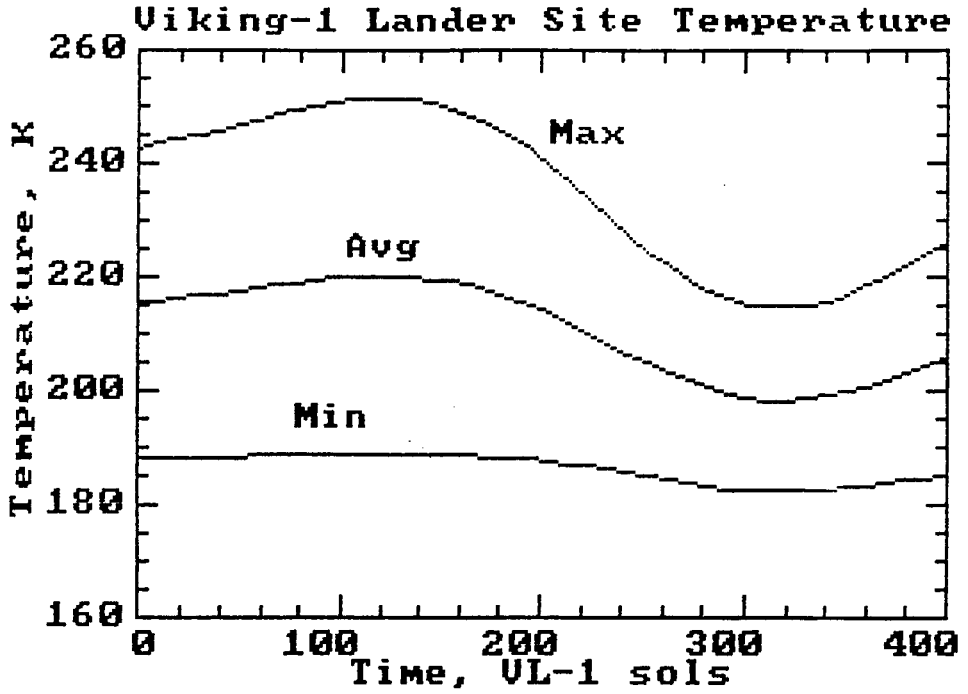

a)

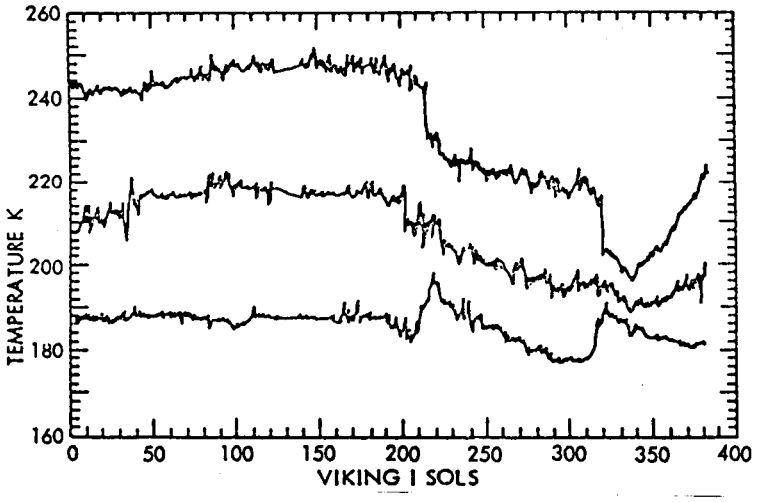

b)

Figure 4 - Seasonal variation of the daily maximum, mean, and minimum temperature at the Viking Lander 1 site (a) computed by MARS-GRAM, and (b) as reported by Ryan and Henry (1979).

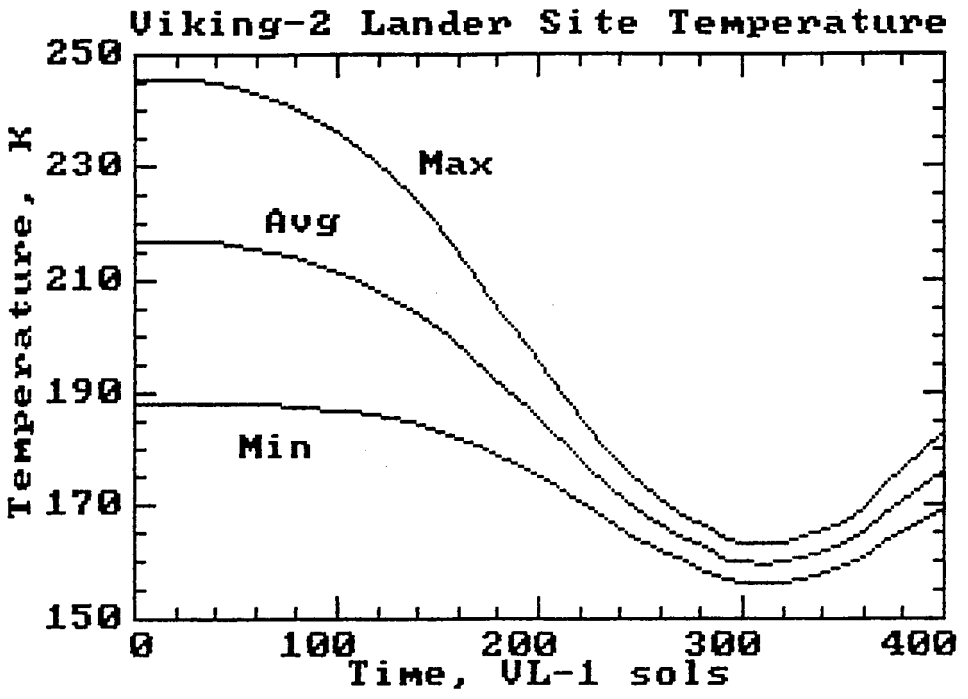

a)

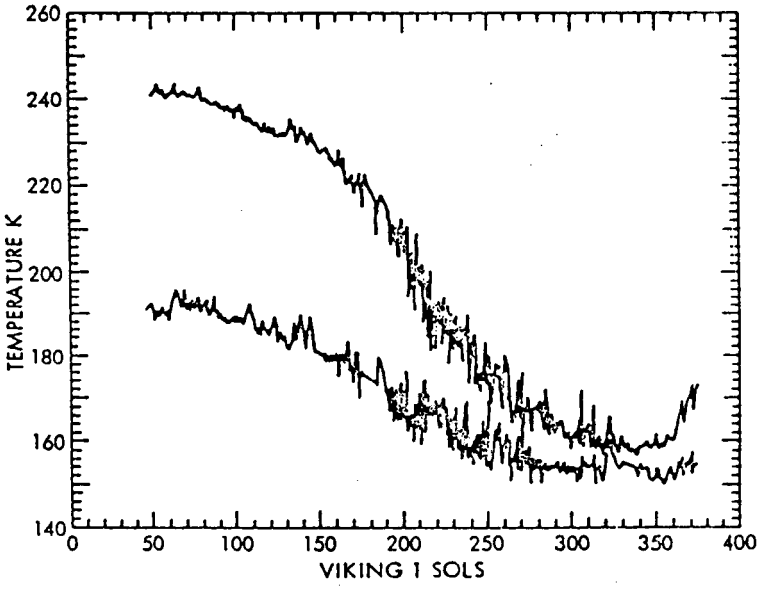

b)

Figure 5 - Seasonal variation of the daily maximum, mean, and minimum temperature at the Viking Lander 2 site (a) computed by MARS-GRAM, and (b) as reported by Ryan and Henry (1979).

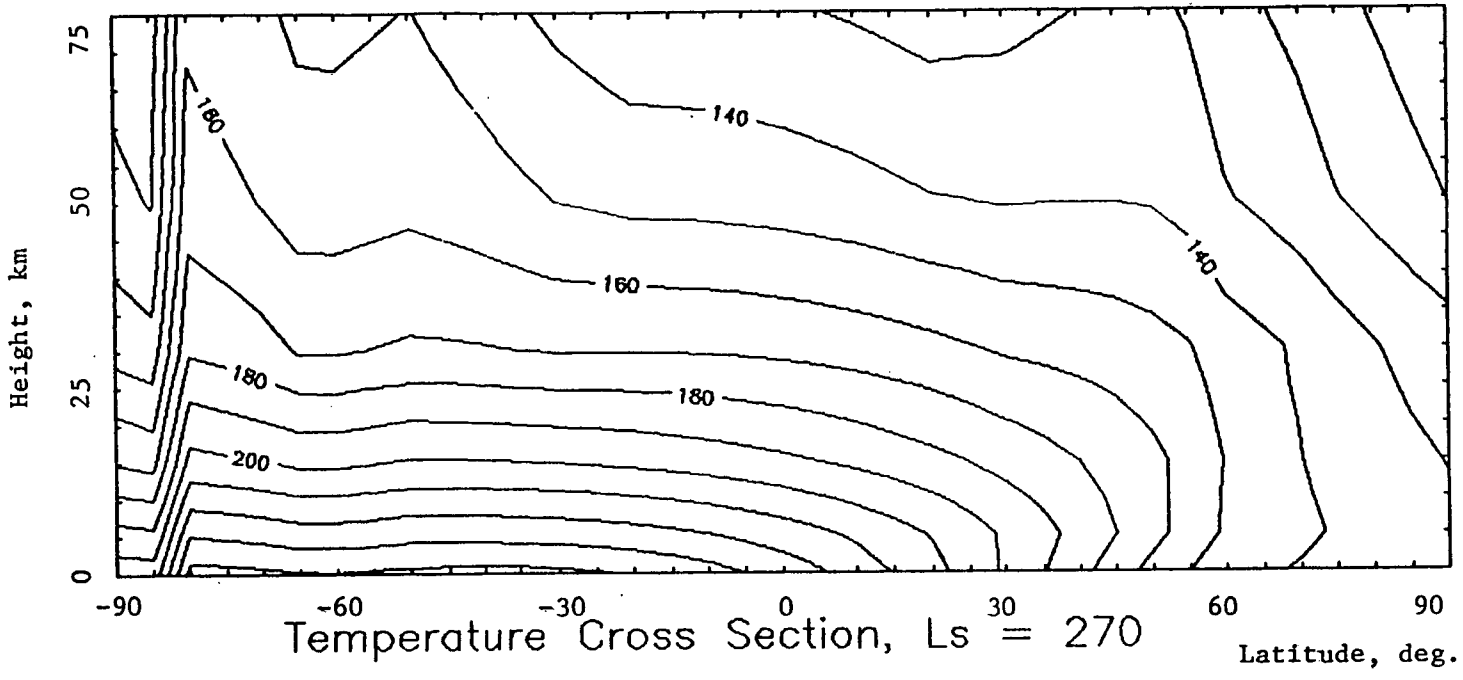

Figure 6 - Height and latitudinal variation of daily mean temperature at Northern Hemisphere winter solstice (areocentric longitude of sun = 270°) for dust-free conditions, computed by MARS-GRAM.

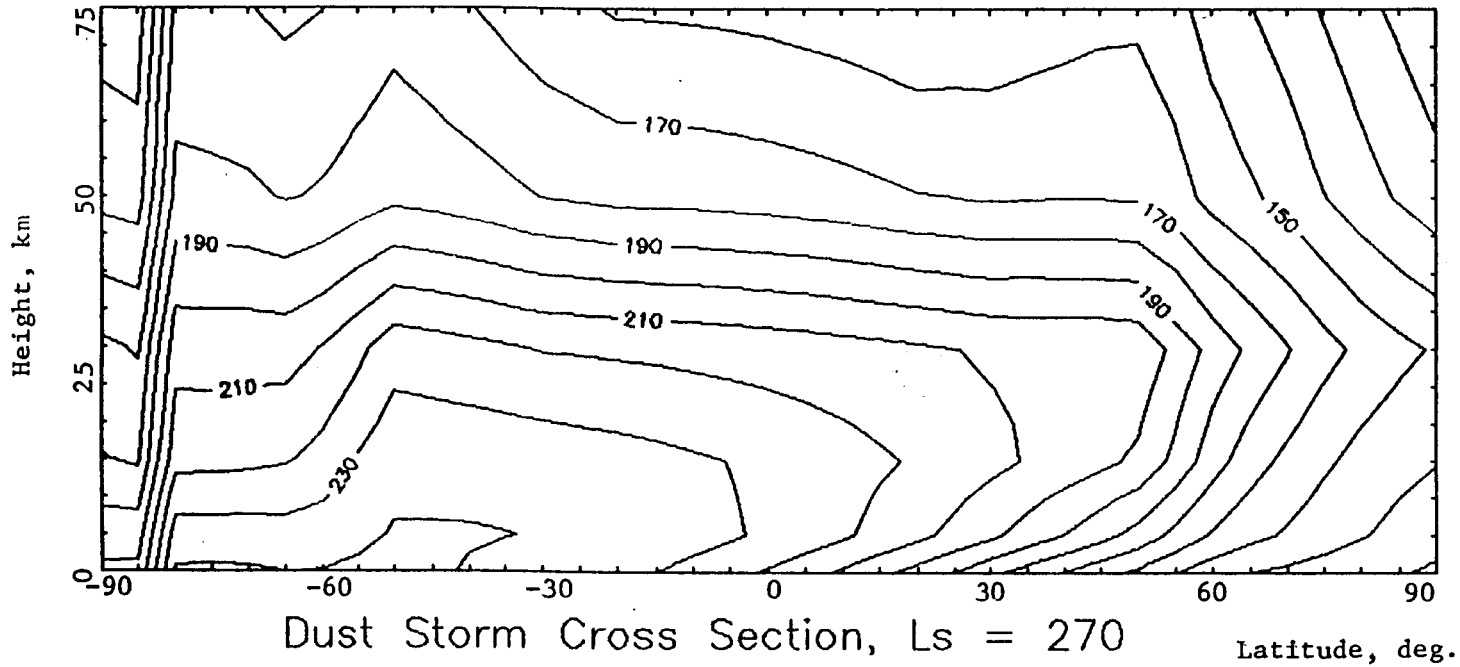

Figure 7 - Height and latitudinal variation of daily mean temperature at Northern Hemisphere winter solstice for a fully-developed global dust storm, computed by MARS-GRAM.

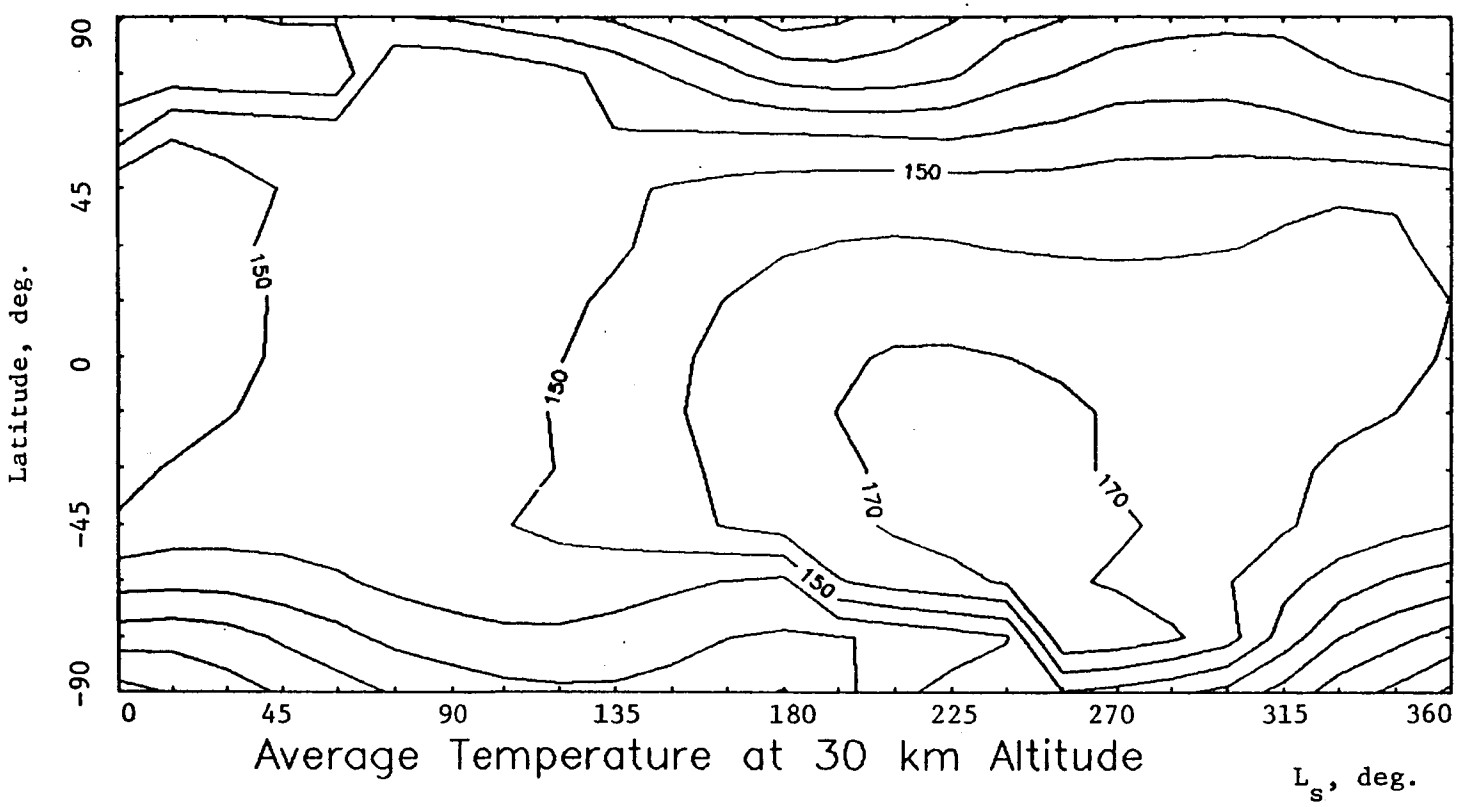

Figure 8 - Seasonal and latitudinal variation of daily average temperature at a height of 30 km, computed by MARS-GRAM.